



THE UNIVERSITY *of* EDINBURGH

Edinburgh Research Explorer

Impact of Biomass Burning emission on total peroxy nitrates: fire plume identification during the BORTAS campaign

Citation for published version:

Aruffo, E, Biancofiore, F, Di Carlo, P, Busilacchio, M, Verdecchia, M, Tomassetti, B, Dari-salisburgo, C, Giammaria, F, Bauguitte, S, Lee, J, Moller, S, Hopkins, J, Punjabi, S, Andrews, S, Lewis, AC, Palmer, PI, Hyer, E, Le Breton, M & Percival, C 2016 'Impact of Biomass Burning emission on total peroxy nitrates: fire plume identification during the BORTAS campaign' pp. 1-28. <https://doi.org/10.5194/amt-2016-45>

Digital Object Identifier (DOI):

[10.5194/amt-2016-45](https://doi.org/10.5194/amt-2016-45)

Link:

[Link to publication record in Edinburgh Research Explorer](#)

Document Version:

Publisher's PDF, also known as Version of record

Publisher Rights Statement:

c Author(s) 2016. CC-BY 3.0 License.

General rights

Copyright for the publications made accessible via the Edinburgh Research Explorer is retained by the author(s) and / or other copyright owners and it is a condition of accessing these publications that users recognise and abide by the legal requirements associated with these rights.

Take down policy

The University of Edinburgh has made every reasonable effort to ensure that Edinburgh Research Explorer content complies with UK legislation. If you believe that the public display of this file breaches copyright please contact openaccess@ed.ac.uk providing details, and we will remove access to the work immediately and investigate your claim.





Impact of Biomass Burning emission on total peroxy nitrates: fire plume identification during the BORTAS campaign

Eleonora Aruffo^{1,2}, Fabio Biancofiore^{1,2}, Piero Di Carlo^{1,2}, Marcella Busilacchio¹, Marco Verdecchia^{1,2}, Barbara Tomassetti^{1,2}, Cesare Dari-Salisburgo¹, Franco Giammaria¹, Stephane Bauguitte³, James Lee⁴, Sarah Moller⁴, James Hopkins⁴, Shalini Punjabi⁴, Stephen Andrews⁴, Alistair C. Lewis⁴, Paul I. Palmer⁵, Edward Hyer⁶, Michael Le Breton⁷, Carl Percival⁷

[1] Center of Excellence CETEMPS, Università dell'Aquila, Via Vetoio, Coppito, L'Aquila, Italy,

[2] Department of Physical and Chemical Sciences, University of L'Aquila, Coppito L'Aquila, Italy,

[3] Facility for Airborne Atmospheric Measurements, Bedfordshire, UK,

[4] Department of Chemistry, University of York, York, UK,

[5] School of GeoSciences, University of Edinburgh, UK.

[6] Marine Meteorology Division, Naval Research Laboratory, Monterey, California, USA.

[7] The Centre for Atmospheric Science, School of Earth, Atmospheric and Environmental Science, University of Manchester, UK.

Correspondence to: E. Aruffo (eleonora.aruffo@aquila.infn.it)

Abstract

The total peroxy nitrates (Σ PNs) concentrations have been measured using a thermal dissociation laser induced fluorescence (TD-LIF) instrument during the BORTAS campaign, which focused on the impact of boreal biomass burning emissions on air quality in the Northern hemisphere. The strong correlation observed between the Σ PNs concentrations and those of the carbon monoxide (CO), a well-known pyrogenic tracer, suggests the possible use of the Σ PNs concentrations as marker of the biomass burning (BB) plumes. We applied both statistical and percentile methods to the Σ PNs concentrations, comparing the percentage of BB plume selected using these methods with the percentage evaluated applying the approaches usually used in literature. Moreover, adding the pressure threshold (~ 750 hPa) to Σ PNs, HCN and CO, as ancillary parameter, the BB plume identification is improved. An artificial recurrent neural network (ANN) model was adapted to simulate the concentrations of Σ PNs and the HCN including as input parameters Σ PNs, HCN, CO and atmospheric pressure, to verify the specific role of these input data to better identify BB plumes.



1. Introduction

Biomass burning (BB) events are an important source of many trace gases and particles in the atmosphere [Crutzen et al., 1979; Crutzen and Andreae, 1990; Goode et al., 2000; Andreae and Merlet, 2001,]. The signature of BB emission in a plume detected far away from the fire is usually the increase of the atmospheric concentration of pyrogenic species including carbon dioxide (CO₂), carbon monoxide (CO), methane (CH₄) and a series of volatile organic compounds (VOCs), accompanied by elevated concentrations of peroxyacyl nitrate (PAN) [e.g., Goode et al., 2000; Cofer et al., 1998; Bertschi et al., 2004; Dibb et al., 2003; Lewis et al., 2007; Tereszchuk et al 2011].

In recent years, several studies have focused on boreal forest fires to quantify the influence of boreal fire emissions on the Earth-Atmosphere system and subsequent impact on the climate. Boreal forest fires (<http://www.borealforest.org>) affect mainly Siberia, Canada and Alaska and occur generally from May to October (Lavoué et al., 2000). In the past three decades occurrence of boreal forest fires and areas burned over Canada have both increased (Gillett et al., 2004; Rinsland et al., 2007; Marlon et al., 2008). The impact of boreal BB on atmospheric chemistry is triggered by the large emissions of CO, NO_x (NO + NO₂), nonmethane hydrocarbons (NMHC) and other NO_y species (Alvarado et al., 2010; Parrington et al., 2012): NO_y = NO_x + ΣRONO₂ + ΣRO₂NO₂ + HNO₃ + HONO + 2N₂O₅ + NO₃, where RONO₂ are total alkyl nitrates (known also as ΣANs), RO₂NO₂ are total peroxy nitrates (known also as ΣPNs), HNO₃ is nitric acid, HONO is nitrous acid, N₂O₅ is dinitrogen pentoxide and NO₃ is nitrate radical. These species can influence the formation of O₃ in the Arctic and at the mid latitudes: the role of boreal BB emissions on the O₃ concentration has been studied by several authors showing situations where O₃ concentrations increased and others where it was unaffected (e.g. Wofsy et al., 1992; Jacob et al., 1992; Mauzerall et al., 1996; Wotawa and Trainer, 2000; Val Martin et al., 2006; Real et al., 2007; Leung et al., 2007; Jaffe and Wigder, 2012; Parrington et al., 2012). The formation of NO_x oxidation products (ΣANs, ΣPNs and HNO₃) plays a very important role in controlling the ozone budget as they inhibit local O₃ formation (Leung et al., 2007). Many investigations demonstrated the central role played by the peroxy acetyl nitrate (PAN), one of the most common PNs, in BB plume chemistry and, specifically, in the NO_x oxidation processes (Jacob et al., 1992; Hudman et al., 2007). Alvarado et al. (2010) demonstrated the rapid PAN formation occurring within 1-2 hours after the emissions by a BB plume: the 40% of the NO_x initially emitted by the fires is rapidly converted into PAN and the 20% into NO₃ (particles phase). In aged plumes, PAN can represent up to the 67% of the NO_y budget (Alvarado et al., 2010).

Analysis of chemistry of BB emissions starts with identifying a BB plume; however, previous studies have used multiple different approaches for the identification and classification of BB plumes. Many studies have recognized CO as a pyrogenic species (Crutzen et al., 1979; Andreae and Merlet, 2001;



1 Lewis et al., 2013), but other chemical species, such as HCN and CH₃CN, have also been employed
 2 to identify a BB plume. In the assembly of the BORTAS data analysis, different procedures have
 3 been applied. Palmer et al. (2013) identified a threshold for each of these species that would separate
 4 air masses produced during boreal BB from background air masses; they defined a BB plume when
 5 the CO, hydrogen cyanide (HCN) and acetonitrile (CH₃CN) levels are higher than 148 ppb, 122 ppt
 6 and 150 ppt, respectively. These thresholds correspond to the 99th percentile ($\sim \text{mean} \pm 3\sigma$) of the data
 7 for the species measured during the flight B625, in which there was not a significant correlation
 8 between the CO and the CH₃CN. In the context of the BORTAS campaign, Lewis et al. (2013)
 9 classified the air masses in three groups: 1) background if CO < 200 ppb; 2) BB plumes if the CO >
 10 200 ppb with the presence of pyrogenic species such as furan or furfural; 3) anthropogenic plumes if
 11 CO > 200 ppb with the absence of furan or furfural. Le Breton et al (2013) observed a strong
 12 correlation between the HCN, CO and CH₃CN indicating the utilisation of HCN as a BB marker.
 13 They identified a BB plume using a standard deviation (σ) method applied to the 1 Hz HCN
 14 measurements: when the HCN concentrations were 6 σ above the background for the flights in
 15 analysis, they flagged the air mass as a BB plume. The 6 σ threshold was chosen since it produces the
 16 highest R² values for the correlation between the HCN and the CO. For other experiments different
 17 methods for the BB plumes identification have been suggested: 1) Holzinger et al. (2005) used a
 18 method similar to that used by Le Breton et al. (2013); their results highlighted a good correlation
 19 between acetonitrile (CH₃CN) and CO and they identified BB plumes by significant peaks in the
 20 CH₃CN volume mixing ratio (using a threshold of 3 σ above the background level); 2) Vay et al.
 21 (2011) identified a plume when CO > 160 ppb (the median observed CO concentration at the surface),
 22 CH₃CN > 225 ppt (threshold characterized by an evident enhancement in CH₃CN mixing ratios) or
 23 HCN > 500 ppt (when the CH₃CN was not available); 3) Hornbrook et al. (2011) defined a plume by
 24 elevated fire tracers above the local background using thresholds of CH₃CN > 200 ppt, HCN > 400
 25 ppt and CO > 175 ppb; 4) Tereszchuk et al. (2011) selected as BB plumes air masses when HCN >
 26 350 ppt, assuming that background concentrations of HCN in the free troposphere range between 225
 27 ppt and 250 ppt and, finally, 5) Alvarado et al. (2010) observed the enhancement of CO correlated
 28 with an enhancement in HCN and CH₃CN; they identified a plume as having a CO concentration at
 29 least 20 ppb above the background level.

30 An aircraft campaign was conducted in Nova Scotia (Canada) with the principle purpose of evaluating
 31 the BB emissions impact on tropospheric photochemistry in the Northern Hemisphere. This work is
 32 part of the BORTAS project (quantifying the impact of BOREal forest fires on Tropospheric oxidants
 33 over the Atlantic using Aircraft and Satellites). This project included a field campaign using a
 34 research aircraft (the FAAM BAe-146) conducted in July and August 2011 during the boreal forest



1 fire season in Canada. Further details about this project can be found in Palmer et al. (2013) and at
 2 <http://www.geos.ed.ac.uk/research/eochem/bortas/>.
 3 In our analysis of the BORTAS aircraft measurement data, we found a good correlation between the
 4 Σ PNs and CO, suggesting the potential of Σ PNs as pyrogenic tracer to discriminate the BB plumes.
 5 Therefore, in this work we propose two different methods to use the Σ PNs as BB tracer: a statistical
 6 approach using the 6σ threshold and the 99th percentile of the Σ PNs calculated for the B625 flight.
 7 We evaluated all of the methods described above to our dataset to compare the results of different
 8 methods to identify BB plumes. We show also that, in some cases, the introduction of meteorological
 9 parameters, which take into account of the air masses vertical position in the atmosphere,
 10 discriminates better the origin of the air masses and, then, helps to select more precisely a BB plume.
 11 Finally, in order to refine the method we adapted an artificial neural network model and we used it to
 12 simulate the Σ PNs and the HCN in two different procedures to BB plume identification: 1) using as
 13 inputs the CO, NO, CH₃CN; 2) adding to the inputs also the pressure.

14

15 **2. Experimental**

16 **2.1 TD-LIF measurements: NO₂, Σ PNs, Σ ANs**

17 A detailed description of the BORTAS experiment can be found in Palmer et al. (2013), along with
 18 a description of the FAAM BAe-146 instrumental payload. During BORTAS campaign (Canada,
 19 summer 2011), observations of NO₂, total Σ PNs, Σ ANs, on board the British FAAM BAe 146
 20 research aircraft, were carried out using the TD-LIF (Thermal Dissociation – Laser Induced
 21 Fluorescence) instrument developed at the University of L'Aquila (Italy) (Dari-Salisburgo et al.,
 22 2009; Di Carlo et al., 2013). Briefly, this technique uses direct measurements of NO₂ molecules by
 23 Laser Induced Fluorescence (LIF), whereas Σ PNs, Σ ANs and HNO₃ are thermally dissociated into
 24 NO₂ heating the air sample at 200°C, 400 °C and 550°C, respectively (Day et al., 2002; Di Carlo et
 25 al., 2013).

26

27 **2.2 Ancillary measurements: O₃, CO, VOCs**

28 Table 1 reports a number of the compounds measured on-board the BAe-146 aircraft during the
 29 BORTAS campaign, specifically those used in this analysis. The instrument used to measure O₃ was
 30 a commercial UV absorption system Model 49C (Thermo Environmental Corp.) (Wilson and Birks,
 31 2006). CO was measured using the vacuum ultraviolet (VUV) resonance fluorescence technique. This
 32 type of CO instrument was applied to aircraft measurement by Gerbig et al. (1999). NO was measured
 33 using a single-channel chemiluminescence instrument manufactured by Air Quality Design, Inc.



1 (Colorado, USA, <http://www.airqualitydesign.com/>) (Lee et al. 2009; Reidmiller et al. 2010).
 2 Concentrations of volatile organic compounds (VOCs) ranging from C5 to C12 were measured by an
 3 automatic gas chromatograph system equipped with a mass spectrometer GC-MS (Purvis et al. 2013).
 4 C2-C7 hydrocarbons and C2-C5 oxygenated volatile organic compounds (o-VOCs) including
 5 alcohols, aldehydes, ketones and ethers were obtained by the University of York (UK) using whole
 6 air sampling (WAS) coupled to an automatic gas chromatograph system equipped with a mass
 7 spectrometer and a flame ionization detector (GC-MS/FID) (Hopkins et al. 2003). Measurements of
 8 a suite of volatile organic compounds: CH₃CN, C₃H₆O, C₅H₈, MVK+MACR, C₄H₈O, C₆H₆, C₇H₈,
 9 C₁₀H₁₆ were made by proton transfer reaction mass spectrometry (PTR MS) (Murphy et al. 2010).
 10 Finally, a chemical ionisation mass spectrometer (CIMS) was used for measuring hydrogen cyanide
 11 (HCN) from biomass burning events (Le Breton et al., 2013).

12

13 **Table 1.** List of FAAM BAe-146 instrumental payload and observed compounds used in the analysis
 14 in this paper. A description of the FAAM BAe-146 instrumental payload, with accuracy and detection
 15 limit, is reported in Palmer et al. (2013).

Species	Method	Reference
CO	VUV resonance/fluorescence	Gerbis et al. (1999)
O ₃	UV absorption	Wilson and Birks (2006)
NO ₂ , ΣRO ₂ NO ₂ , ΣRONO ₂ , NO _y	TD-LIF	Dari-Salisburgo et al. (2009); Di Carlo et al. (2013)
NO	AQD chemiluminescence	Lee et al. 2009; Reidmiller et al. 2010
C ₅ –C ₁₂ VOCs	GC-MS	Purvis et al. (2013)
C ₂ –C ₇ NMHCs, acetone CH ₃ OH	WAS-GC	Hopkins et al. (2003)
HCN	CIMS	Le Breton et al. (2013)



CH ₃ CN, C ₃ H ₆ O, C ₅ H ₈ , MVK+MACR, C ₄ H ₈ O, C ₆ H ₆ , C ₇ H ₈ , C ₁₀ H ₁₆	PTR-MS	Murphy et al. (2010)
---	--------	----------------------

3. Plume identification

Figure 1 shows the time series of the species investigated in this paper (Σ PNs, acetonitrile, HCN, CO and furfural) for one of the flights analysed (B623), illustrated as an example. The Σ PNs trends shows exactly the same structures present on CO and CH₃CN, with the exception of two plumes (in the temporal intervals of $(8.2 - 8.4) \times 10^4$ and $(8.6 - 8.8) \times 10^4$ seconds After Midnight (A.M.)) that are extensively analysed in the next sections. Moreover, the furfural shows similar trend for the first part of the flight; since CO, acetonitrile, HCN and Furfural are a known BB tracers (Lewis et al. 2013; Palmer et al. 2013; Le Breton et al., 2013), the significant correlation between the Σ PNs and those species suggests that the Σ PNs also originated at the same boreal biomass burning source and that it can be used as additional chemical species for the identification of the BB plumes.

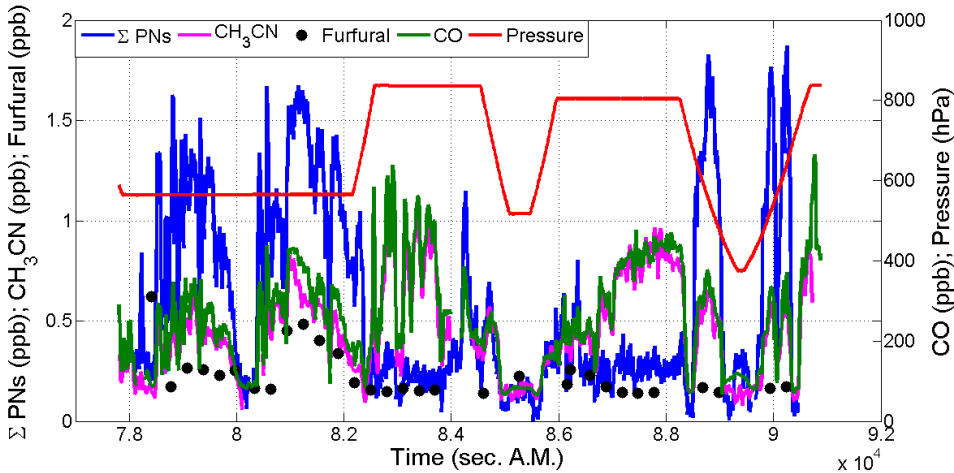


Figure 1. Time series of Σ PNs, CH₃CN, Furfural, CO and pressure during the flight B623, shown as example.



1 As described in the introduction, recently different compounds (CO, HCN or CH₃CN) and different
 2 concentrations thresholds have been introduced as tracers to establish if the air mass monitored is
 3 affected by forest fire emissions or not. These methods are summarized in Table 2.

4 **Table 2.** Methods to identify BB plumes.

	Methods
Holzinger et al. (2005)	CH ₃ CN > 3σ
Alvarado et al. (2010)	CO increase of at least 20 ppb respect to the background and its correlation with HCN or CH ₃ CN
Vay et al. (2011)	CO > 160 ppb, HCN > 500 ppt or CH ₃ CN > 225 ppt
Hornbrook et al. (2011)	CO > 175 ppb, HCN > 400 ppt, CH ₃ CN > 200 ppt
Tereszczuk et al. (2011)	HCN > 350 ppt
Lewis et al. (2013)	CO > 200 ppb and presence of furan or furfural
Palmer et al. (2013)	CO > 148 ppb, HCN > 122 ppt and CH ₃ CN > 150 ppt
Le Breton et al. (2013)	HCN > 6σ
This work	ΣPNs > 6σ or ΣPNs > 418 ppt

5

6 In our analysis we tested the use of the concentration profiles of ΣPNs as possible identifier of BB
 7 plumes. We applied two different methods: 1) evaluating the 99th percentile of the ΣPNs
 8 concentrations measured during the background flight B625 (as done by Palmer et al., 2013) and
 9 using this value as threshold to distinguish air masses emitted by fires; 2) applying the statistical
 10 approach (σ method). In the first case, we calculate the 99th percentile of the 1 second ΣPNs data
 11 sampled during the B625 finding a threshold of 418 ppt. In the second case, first we selected the parts
 12 of each flight identifiable as background and, then, we evaluated for these data the mean and the
 13 standard deviation of the ΣPNs; after that, we identified as BB plumes the parts of each flight in
 14 which the difference between ΣPNs concentrations and the background level were higher than 6
 15 standard deviations of the background. This threshold has been evaluated calculating the correlation
 16 coefficients between the ΣPNs and the CO varying the sigma threshold between 10σ and 3σ for each
 17 flight in which the ΣPNs showed evident and clear plumes (such as B622 and B623): we found that
 18 the maximum R occurred when we selected the BB plume using the 6σ threshold. In Table 3 are
 19 summarized the correlation coefficients R and the percentage of flight selected as BB plume obtained
 20 for all the flights in analysis using both the methods just described. Moreover, we indicated the
 21 percentage of flight identified as BB plume applying all the methods listed in Table 2 to our dataset.



1

2 **Table 3.** Correlation coefficient (R) and percentage (%) of each flight of the BORTAS campaign
 3 selected as BB plume using both the Σ PNs methods (6σ and 99th percentile thresholds) and percentage
 4 (%) of BB plume evaluated for each BORTAS flight using the methods applied in other studies.

Flight	This study (Σ PNs methods)				Other studies		
	6σ		Σ PNs > 0.418 99 th percentile				
	R	%	R	%		%	Comments
B619a	-	0	-0.045	13.5	Palmer et al.	0	Only CO
					Vay et al.	0	Only CO
					Hornbrook et al.	0	Only CO
					Holzinger et al.	-	No CH ₃ CN
					Alvarado et al.	1.3	Only CO
					Lewis et al.	0	No Furfural – CO < 200
					Tereszczuk et al.	-	No HCN
					Le Breton et al.	-	No HCN
B619b	-	0	-0.168	1.3	Palmer et al.	0	Only CO
					Vay et al.	0	Only CO
					Hornbrook et al.	0	Only CO
					Holzinger et al.	-	No CH ₃ CN
					Alvarado et al.	0	Only CO
					Lewis et al.	0	No Furfural – CO < 200
					Tereszczuk et al.	-	No HCN
					Le Breton et al.	-	No HCN
B620	-	0	-	0	Palmer et al.	0	Only CO
					Vay et al.	0	Only CO
					Hornbrook et al.	0	Only CO
					Holzinger et al.	-	No CH ₃ CN
					Alvarado et al.	5.1	Only CO
					Lewis et al.	0	No Furfural - CO < 200
					Tereszczuk et al.	-	No HCN
					Le Breton et al.	-	No HCN



B621a	0.953	59.1	0.951	77.6	Palmer et al.	58.9	
					Vay et al.	23.1	
					Hornbrook et al.	32.5	
					Holzinger et al.	72.3	
					Alvarado et al.	76.8	
					Lewis et al.	-	No Furfural – CO > 200
					Tereszczuk et al.	41.6	
					Le Breton et al.	47.7	
B621b	0.644	3.6	0.644	3.6	Palmer et al.	2.0	NO CH ₃ CN in the plume; missing data of HCN in the flight (only a plume)
					Vay et al.	0	NO CH ₃ CN in the plume; missing data of HCN in the flight (only a plume)
					Hornbrook et al.	0	NO CH ₃ CN in the plume; missing data of HCN in the flight (only a plume)
					Holzinger et al.	0.6	Missing data for the CH ₃ CN in the flight
					Alvarado et al.	14.4	
					Lewis et al.	-	No Furfural – CO > 200
					Tereszczuk et al.	26.3	
					Le Breton et al.	32.4	Missing data (only a plume)
B622	0.867	51.9	0.864	55.8	Palmer et al.	52.2	
					Vay et al.	7.2	
					Hornbrook et al.	10.7	
					Holzinger et al.	50.0	
					Alvarado et al.	74.2	
					Lewis et al.	45.6	



					Tereszczuk et al.	10.4	
					Le Breton et al.	51.1	
B623	0.804	41.2	0.776	42.6	Palmer et al.	76.9	No HCN
					Vay et al.	73.6	No HCN
					Hornbrook et al.	70.5	No HCN
					Holzinger et al.	80.5	
					Alvarado et al.	85.6	
					Lewis et al.	71.0	
					Tereszczuk et al.	-	No HCN
					Le Breton et al.	-	No HCN
B626a	-	0	-	0	Palmer et al.	0	No HCN
					Vay et al.	0	No HCN
					Hornbrook et al.	0	No HCN
					Holzinger et al.	0.6	
					Alvarado et al.	2.0	
					Lewis et al.	0	No Furfural – CO < 200
					Tereszczuk et al.	-	No HCN
					Le Breton et al.	-	No HCN
B626b	0.755	8.1	0.259	0.4	Palmer et al.	8.6	No CH ₃ CN
					Vay et al.	5.6	No CH ₃ CN
					Hornbrook et al.	3.7	No CH ₃ CN
					Holzinger et al.	-	No CH ₃ CN
					Alvarado et al.	8.5	
					Lewis et al.	1.9	
					Tereszczuk et al.	15.1	
					Le Breton et al.	19.3	
B627	-	0	0.073	11.0	Palmer et al.	0	No HCN
					Vay et al.	0	No HCN
					Hornbrook et al.	0	No HCN
					Holzinger et al.	0.3	
					Alvarado et al.	3.1	
					Lewis et al.	0	No Furfural – CO < 200
					Tereszczuk et al.	-	No HCN

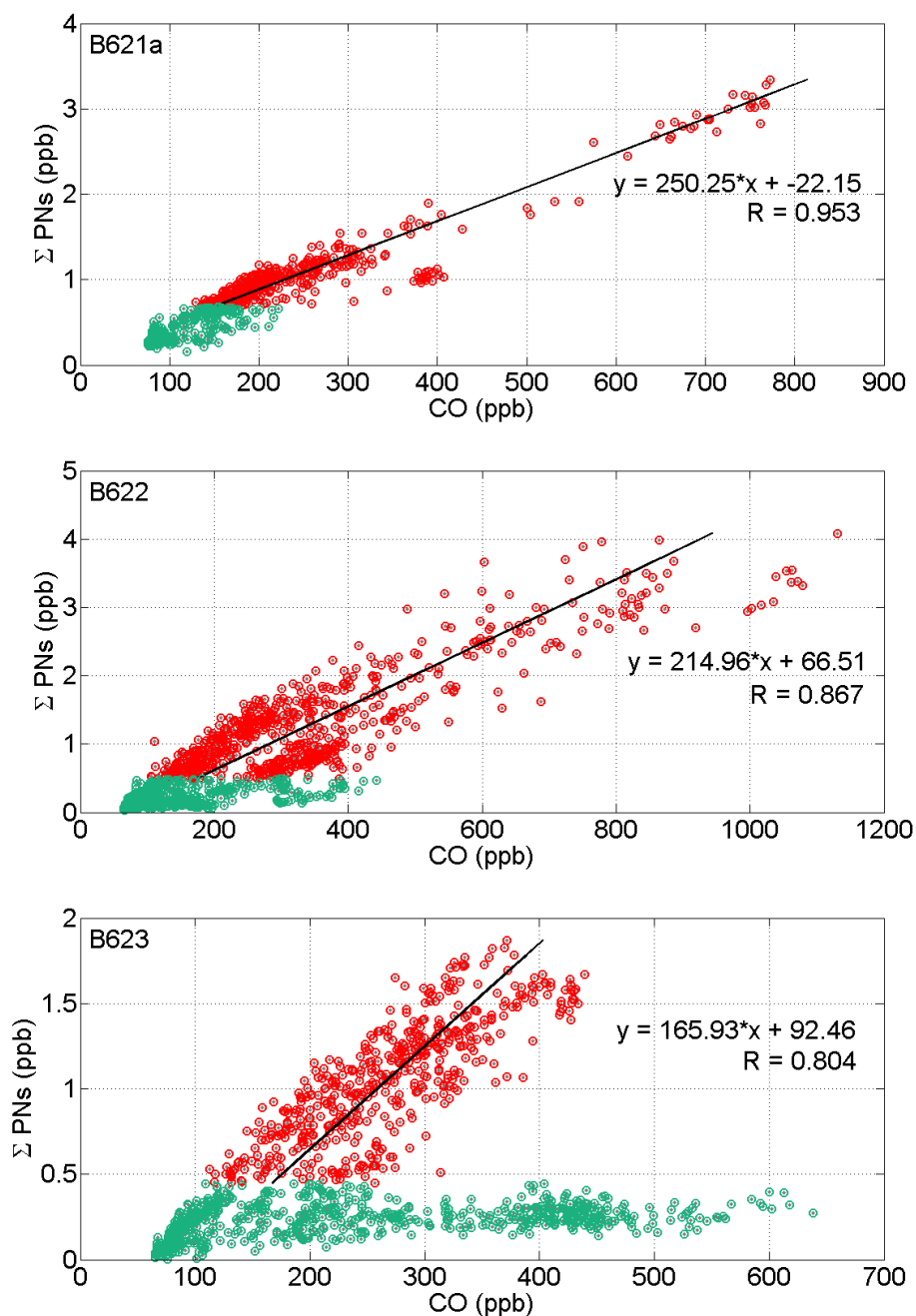


					Le Breton et al.	-	No HCN
B628a	-	0	-	0	Palmer et al.	0	
					Vay et al.	0	
					Hornbrook et al.	0	
					Holzinger et al.	0.3	
					Alvarado et al.	21.0	
					Lewis et al.	0	No Furfural – CO < 200
					Tereszczuk et al.	0	
					Le Breton et al.	40.1	
B628b	0.477	11.9	0.540	10.6	Palmer et al.	2.5	No HCN
					Vay et al.	0	No HCN
					Hornbrook et al.	0	No HCN
					Holzinger et al.	6.3	
					Alvarado et al.	61.1	
					Lewis et al.	0	No Furfural – CO < 200
					Tereszczuk et al.	-	No HCN
					Le Breton et al.	-	No HCN
B629	-0.036	6.4	-0.010	5.7	Palmer et al.	3.9	No HCN
					Vay et al.	1.1	No HCN
					Hornbrook et al.	0	No HCN
					Holzinger et al.	7.6	
					Alvarado et al.	6.2	
					Lewis et al.	0	No Furfural – CO < 200
					Tereszczuk et al.	-	No HCN
					Le Breton et al.	-	No HCN
B630	0.007	2.0	0.005	2.6	Palmer et al.	12.0	No HCN
					Vay et al.	5.1	No HCN
					Hornbrook et al.	2.4	No HCN
					Holzinger et al.	26.2	
					Alvarado et al.	42.9	
					Lewis et al.	-	No Furfural – peak with CO > 200
					Tereszczuk et al.	-	No HCN



					Le Breton et al.	-	No HCN
--	--	--	--	--	------------------	---	--------

1
 2 In order to make the analysis as accurate as possible, the double flights were separated and applied
 3 all the methods in each part of the flights taking into account of different Canadian regions and
 4 different hours of the day during which we were flying. The Σ PNs methods give, in most cases,
 5 results in agreement with each of the methods that use CO, HCN and CH₃CN (see table 3) and allow
 6 to discriminate 3 flights (B621a, B622 and B623) in which a significant percentage (higher than the
 7 40% with R ranging between 0.804 and 0.953) of the data have been collected sampling air masses
 8 emitted by biomass burning. Moreover, these results are also in agreement with what is found
 9 applying the approaches suggested in other studies. We found three flights (B621b, B626b and
 10 B628b) in which the majority of the methods show that a small percentage (less than 10% with R
 11 ranging between 0.477 and 0.755) of data can be identified as BB plumes (see table 3). In six flights
 12 (B619a, B619b, B620, B626a, B627 and B628a) the Σ PNs 6 σ method suggests, in agreement with
 13 the majority of the other techniques, a dominance of background air masses sampled; the 99th
 14 percentile method applied to the Σ PNs for the flights B619a, B619b and B627 show a small fraction
 15 of flight selected as BB. Moreover, the R values between the Σ PNs and the CO in those points is so
 16 low (or even negative) to suggest that these parts of the flights are not ascribable as BB plume. The
 17 flights B629 and B630 present a small percentage of the flight identified as BB plume, using the
 18 Σ PNs methods (confirmed also by other methods), but the low (or negative) R values suggest a
 19 different origin for these plumes. Summarizing, we classified three flights (highlighted in grey in
 20 Table 3) with evidence of significant BB plumes sampled, three with a small percentage of BB plumes
 21 and 8 flights with a dominance of background air masses sampled. Le Breton et al. (2013) evaluated
 22 the percentage of flights ascribable as BB plumes using the 6 σ method applied to their HCN
 23 measurements and the R² between the CO and the HCN in the BB plumes for five flights. Our results,
 24 with the percentage of flight identified as BB plume using their method, are in agreement with those
 25 that they presented, with the exception of the B621 flight. In this case, the difference could be due to
 26 the fact that we split the double flights into two datasets and also because for the B621b there are
 27 some missing data for the HCN and only one big plume. Moreover, the R² between HCN and CO
 28 range between 0.46 (B622) and 0.83 (B621) (Le Breton et al., 2013).
 29 Figure 2 shows the scatter plot between the Σ PNs and the CO for the flights B621a, B622 and B623:
 30 the red circles are the BB plume selected by the 6 σ of the Σ PNs technique and the green circles the
 31 background part of each flight



1 **Figure 2.** Scatter plot between the ΣPNs and the CO for the B621a, B622 and B623 flights (from the
 2 top to the bottom, respectively). The red points indicate the data selected as BB plume using the 6σ
 3 method to the ΣPNs measurements, the green points indicate the background air masses.



1 The Σ PNs show a very good correlation with the CO, in presence of BB plumes: the correlation
 2 coefficients R , in fact, vary between 0.804 and 0.953. The data of the B623 flight (Figure 2) show an
 3 interesting, well distinct double trends between the Σ PNs and the CO; the time series (Figure 1)
 4 shows that the CO and the CH_3CN present two plumes (between 8.2×10^4 - 8.4×10^4 seconds A.M. and
 5 between 8.6×10^4 - 8.8×10^4 seconds A.M.) at pressure (P) higher than ~ 750 hPa (corresponding to an
 6 altitude of ~ 2000 m a.s.l.): at these plumes do not correspond an increase of the Σ PNs nor of the
 7 Furfural. In order to explain the double trends in the Σ PNs vs CO scatter plot of the flight B623 (see
 8 figure 2), we analysed the all dataset of this flight as function of the pressure, finding that the two
 9 trends can be distinguished using a pressure threshold of 750 hPa (Figure 3), or equivalently an
 10 altitude threshold of ~ 2000 m a.s.l. (not shown).

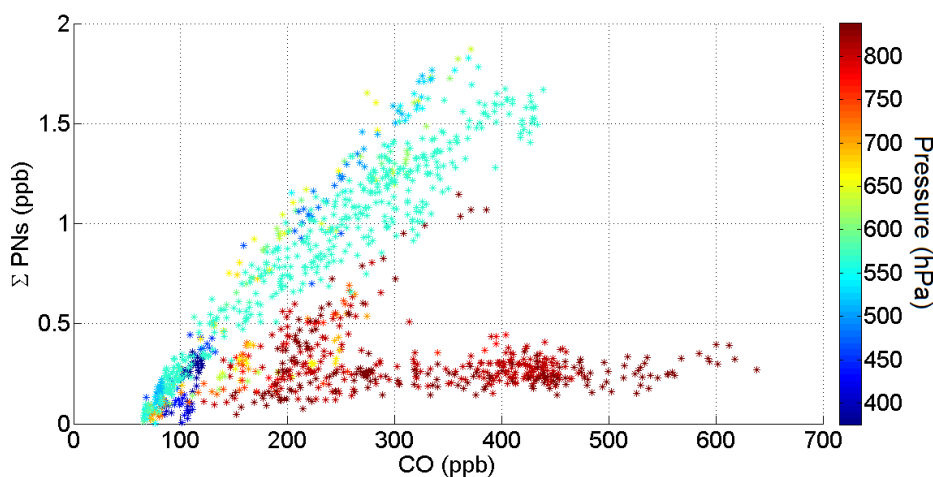
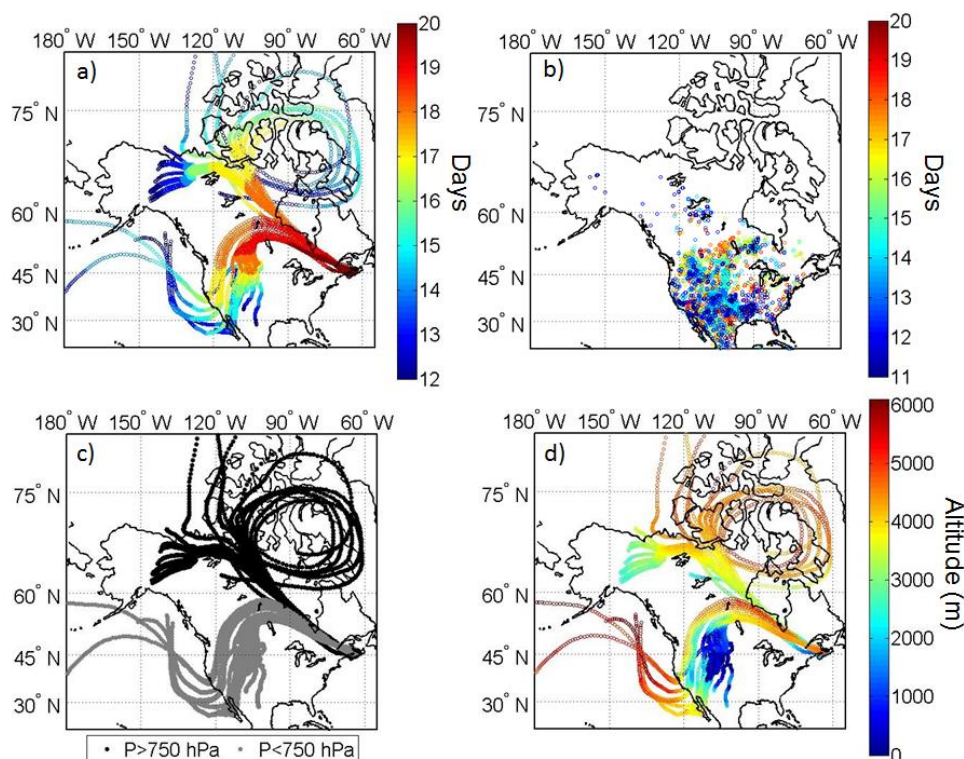


Figure 3. Scatter plot between the Σ PNs and the CO as function of the pressure of the flight B623.

14 The fact that the two distinct trends of the flight B623 are separable by the 6σ method of the Σ PNs
 15 and by pressure, suggests that the air masses sampled at different altitude are originated by different
 16 sources, and the smaller correlation ($R = 0.31$) between Σ PNs and CO for pressure above 750 hPa,
 17 supports the hypothesis that they are not impacted by BB emission. To prove this thesis, we evaluated
 18 the lagrangian back-trajectories (Hysplit model, Draxler et al., 1999) selecting the starting point at
 19 different altitudes along the flight trajectory and running the model up to 200 hours back. Panel c) in
 20 Figure 4 shows the black-trajectories of air masses sampled at pressure higher than 750 hPa (black
 21 points) or lower than 750 hPa (grey points): a different origin is clearly identifiable. In particular, air
 22 masses collected at lower altitudes ($P > 750$ hPa) come from the northern region of the Canada and
 23 the altitude of provenience increases the further back the trajectory goes and decreases in the last
 24 three days of simulation (Figure 4d); on the contrary the air masses corresponding to $P < 750$ hPa



1 originated in the South-West region of the Canada (e.g., Alberta, Saskatchewan,...) and in the North-
 2 West states of the U.S.A. (e.g., Montana, Idaho, Wyoming, Washington, Oregon,...). Figure 4a
 3 represents the position of the air masses along the back-trajectories during the days between the July
 4 12th and July 20th (corresponding respectively to -200 hours back and 0 hours back in the back-
 5 trajectories model setup). In the same way, Figure 4b shows the fire spots recorded by the FLAMBE
 6 (The Fire Locating And Monitoring of Burning Emissions, Reid et al., 2009) archives as function of
 7 the day in which the biomass burning occurred (between the July 11th and July 20th). The Figure 4
 8 reveals not only that air masses collected for $P > 750$ hPa come from a different region of the North
 9 America respect to those collected for $P < 750$ hPa, but also that the regions of interest for air masses
 10 at $P > 750$ hPa are, most likely, not impacted by fire emissions, at least for the days in which the air
 11 masses passed over those areas. On the contrary, the plumes (identified as BB plumes) measured at
 12 $P < 750$ hPa (i.e. altitude higher than 2000 m a.s.l.) have originated from regions strongly influenced
 13 by biomass burning fires (see panel b of figure 4) in the central-west coast of the North America)
 14 in the days of July in which the air masses flew above those territories. The back-trajectories analysis,
 15 therefore, confirm the existence of two different layers of air masses sampled during the B623 flight
 16 distinguishable by the pressure (i.e. the altitude).



17



1 **Figure 4.** Panel a): temporal position (express as day from the 12th July to the 20th of July) along the
 2 200 hours back-trajectories. Panel b): spot of the biomass burning fires derived from the FLAMBE
 3 archive as function of the day in which they occurred (from 11th July to 20th July – we selected the
 4 dataset at the 13.00 UTC and the 23.00 UTC). Panel c): distinction of the back trajectories position
 5 selecting the starting point along the flight trajectories for $P \geq 750$ hPa. Panel d): altitude along the
 6 back trajectories.

7
 8 Finally, we evaluated the qualitative age of the air masses sampled during the B623 flight: using the
 9 ratio between the NO_x (sum of the TD-LIF NO₂ and the chemiluminescence NO measurements) and
 10 the total NO_y (measured by the TD-LIF and the calculated as sum of NO_x and its oxidation products),
 11 we observed that the air masses sampled at $P < 750$ hPa are younger respect those sampled at higher
 12 pressure confirming that the air masses identifiable by the pressure are distinct not only for their
 13 sources (and provenience), but also for the age.

14 Considering what has been highlighted analysing the double trends in the CO vs Σ PNs plot of the
 15 B623, we examined in depth the correlation between the CO and the Σ PNs for all the flights and we
 16 found that also other flights show similar trends: in fact, B621a and the B622 show two different
 17 trends that can be distinguished using a pressure threshold of 700 hPa (figure not shown). Moreover,
 18 we did the same analysis also for the HCN: we found that for the B621a, B622 the scatter plot (plotting
 19 only the data selected as BB plume using the Le Breton et al. (2013) method) between the HCN and
 20 the CO shows different trends that can be distinct by the pressure (Figure 5, panel a and b related to
 21 the B621a and B622 flight, respectively). This analysis suggest that, even though the identification
 22 of a BB plume done using different chemical species threshold is largely and successfully employed
 23 (Le Breton et al., 2013; Lewis et al., 2013; Palmer et al., 2013; O'Shea et al. 2013), there are some
 24 episodes in which the introduction of other parameters (such as the pressure or the altitude, which are
 25 indicative of the vertical position of the air masses and, therefore, may be particularly significant for
 26 observations on-board aircrafts) gives interesting information and allow to discriminate better and
 27 with more details the plumes. The back-trajectories evaluation also gives an important indication of
 28 the origin of the air masses and completes the analysis.

29

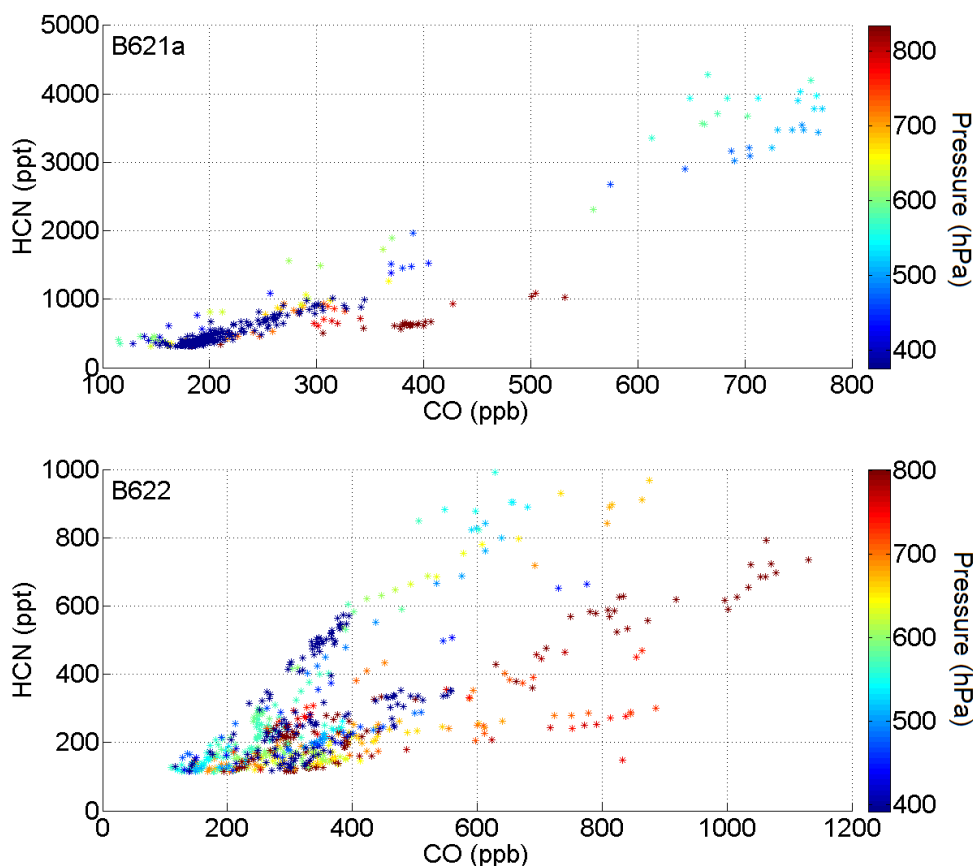


Figure 5. Scatter plot between the HCN and the CO as function of the pressure for the flights B621a (at the top) and B622 (at the bottom).

4. Model results

In order to refine the methods to discriminate the BB plumes and better understand the origin of the air masses analysed in the BORTAS campaign, an artificial neural network (ANN) model, recently developed for O₃ and PM studies (Biancofiore et al., 2015a; Biancofiore et al., 2015b), has been adapted and used with BORTAS dataset. The ANN is capable of simulating non-linear relationships (Lonbladd et al. 1992) and for this reason is ideal for investigating the relationship between Σ PNs (and HCN) and chemical and physical parameters. In this work, a recurrent architecture was used (Elman, 1990) that provides a multi-step memory. We simulated the concentrations of the Σ PNs for the B623 flight and of the Σ PNs and the HCN for the B622. During both these flights the scatter plots between the Σ PNs and the CO or the HCN and the CO show different trends that we distinguished by the pressure and that are indicative of air masses having different origins (coming from regions



1 interested by fires or not), as explained in Section 3. We carried out two different simulations: a) we
 2 used as input for the neural network only the O₃, CO, NO and CH₃CN (case A); b) we used as input
 3 the O₃, CO, NO, CH₃CN and the pressure (case B). In this way, we evaluated if and how the
 4 simulations of the Σ PNs and the HCN change by adding a physical parameter to the inputs, therefore
 5 taking into account the position of the air masses (that is the altitude of the aircraft during the flights).
 6 Figure 6 shows the results of the case A simulations for the flight B622: the scatter plot between the
 7 simulated HCN (panel a) and Σ PNs (panel b) and the measured CO as function of the pressure does
 8 not present distinct trends as evident in the measured data. Similar results have been found for the
 9 case A simulations (panel c in Figure 6) of the flight B623: the net separation of two trends in the
 10 Σ PNs vs CO scatter plot of the measured data (Figure 2) is not reproduced by the model. On the
 11 contrary, adding the pressure to the inputs (case B) the simulations improve significantly for both the
 12 flights and both the species; Figure 7 shows the ANN simulations in the case B. It is evident that the
 13 different trends, identifiable by the pressure using the measured data (Figure 3 and Figure 5), are well
 14 reproduced and become evident despite what occurred in the case A (Figure 6). Moreover, it is clear
 15 also that the correlation coefficients between the Σ PNs measured and the Σ PNs simulated increase
 16 adding the pressure to the inputs (these results are highlighted in grey in Table 4): in fact, R improves
 17 from 0.94 (case A) to 0.95 (case B) for the B622 flight and, even more, from 0.77 (case A) to 0.94
 18 (case B) for the flight B623, in which the two trends between the Σ PNs and the CO is significantly
 19 more evident respect to the B622 flight. Similar results can be found for the HCN: the correlation
 20 coefficient R, in fact, increases from 0.86 (case A) to 0.92 (case B). In addition to the correlation
 21 coefficient R, we estimated the model performances using three more typical indices (Biancofiore et
 22 al., 2015): the fractional bias (FB), the normalized mean squared error (NMSE) and the factor of 2
 23 (FA2). The results are summarized in Table 4. The FB is calculated as the ratio between the difference
 24 of the mean observed and the mean modelled concentrations and their mean; it indicates the systemic
 25 errors that can entail a bias between the modelled and the measured data and can range between -2
 26 (overestimation) and +2 (underestimation): an ideal model has an FB index of 0. The NMSE is the
 27 result of the ratio between the mean of the squared difference between the observed and the modelled
 28 concentrations and the sum of their mean; it gives information about the total errors of the models
 29 and the best value is 0 (as the NMSE decreases approaching 0, the model performance increases).
 30 Finally, the FA2 is the percentage of the simulated data for which the ratio between the observed and
 31 the modelled concentrations is included between 0.5 and 2; the ideal model has an FA2 of 1 and the
 32 worst results occur if FA2 is equal to 0. The Σ PNs simulation for the flight B622 shows that R, NMSE
 33 and the FA2 improve adding the pressure to the inputs (case B); on the contrary, the FB results slightly
 34 worst indicating that the model tends to overestimate the concentrations. The HCN simulation for the



1 flight B622 has better results for all the indices with the exception, also in this case, of the FB which
 2 is lightly greater in the case B than in the case A. Finally, the R, FB and FA2 of the Σ PNs modelled
 3 for the flight B623 show a significant improvement in the case B respect the case A, but the NMSE
 4 presents a worsening suggesting the possibility of an increase in the systemic or random errors.

5
 6 **Table 4.** Indices to evaluate the Model performances. R is the correlation coefficient, FB is the
 7 fractional bias, NMSE is the normalized mean squared error and FA2 the factor of 2. See the text for
 8 a description of these indices

	Simulations	R	FB	NMSE	FA2
Σ PNs (B622)	Case A	0.94	-0.017	0.124	0.755
	Case B	0.95	-0.023	0.099	0.763
HCN (B622)	Case A	0.86	0.009	0.228	0.946
	Case B	0.92	0.014	0.136	0.959
Σ PNs (B623)	Case A	0.77	0.014	0.028	0.771
	Case B	0.94	-8.8e-4	0.079	0.867

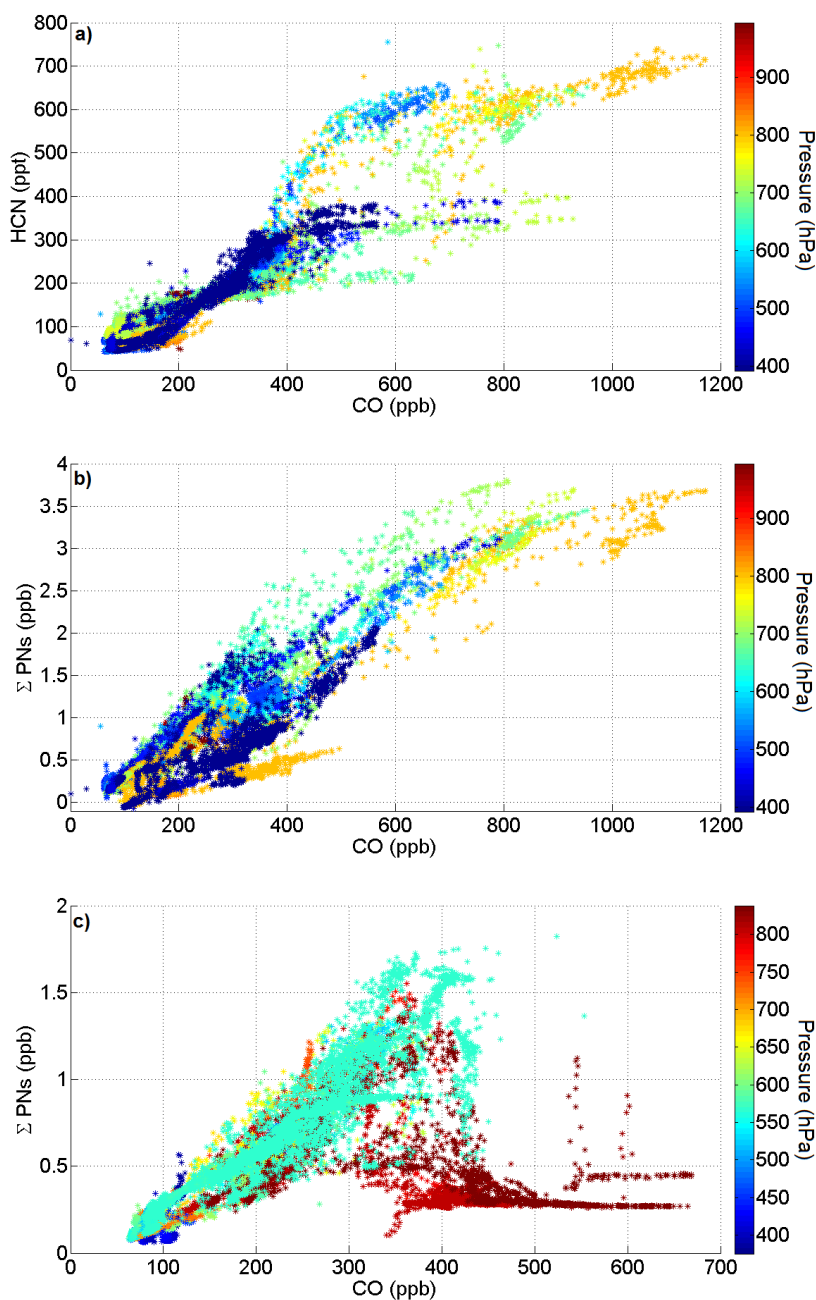
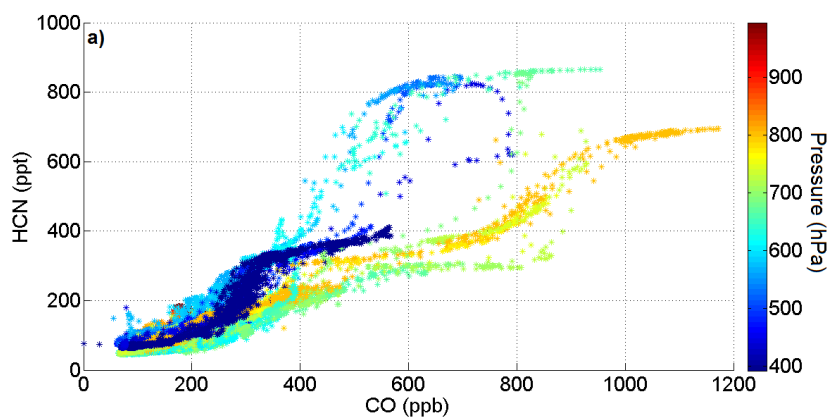
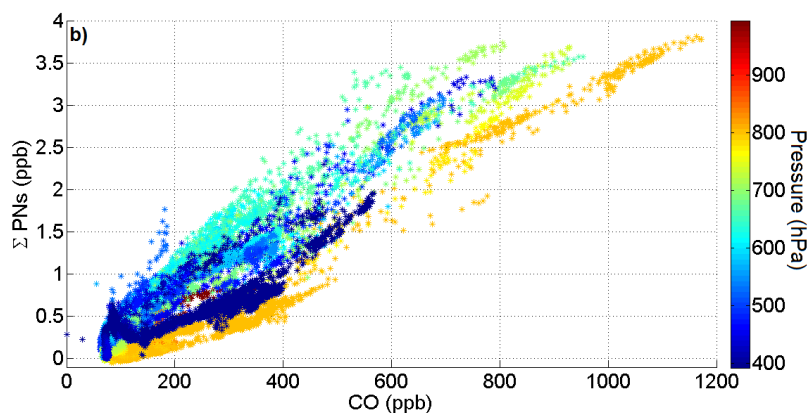


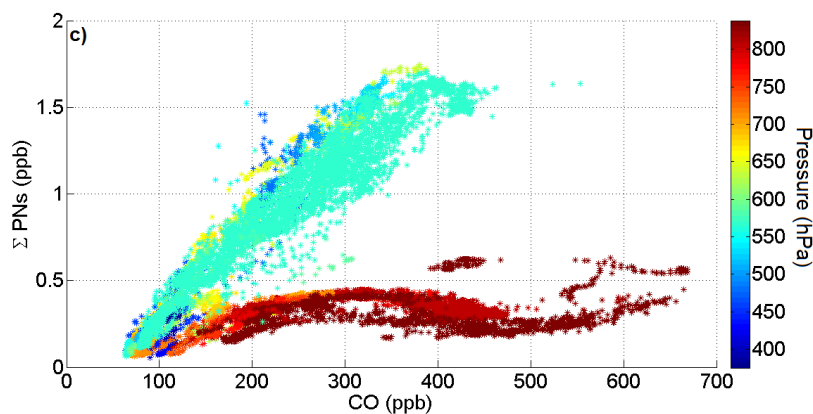
Figure 6. Simulations results for the case A (only O_3 , CO, NO and CH_3CN as inputs): scatter plot between the simulated HCN (panel a)), the simulated Σ PNs (panel b)) and the CO for the B622 and between the simulated Σ PNs and CO for the B622 (panel a)) and the B623 (panel b)).



1



2



3

4 **Figure 7.** Simulations results for the case B (O_3 , CO, NO, CH_3CN and pressure as inputs): scatter
 5 plot between the HCN (panel a)) simulated and the CO for the B622 and between ΣPNs and CO for
 6 the B623 (panel b)).



1 Conclusions

2 The measured Σ PNs during the BORTAS aircraft campaign show a good correlation (R varying
 3 between ~ 0.80 and ~ 0.95) with CO for different flights. We used Σ PNs as BB tracers applying two
 4 different methods to select a BB plumes: 1) we defined a threshold of 6σ of Σ PNs concentration for
 5 each flights and all the data that are 6σ times higher than the background level have been selected as
 6 BB plume; 2) evaluating the 99th percentile of the Σ PNs measurements done during the B625 flight
 7 (considered a background flight not affected by BB plumes). Moreover, we applied several methods
 8 present in the literature to our dataset to compare with the proposed Σ PNs methods and we calculated
 9 the percentage of flight classifiable as BB plume; we found that all the methods identified four flights
 10 with evident and significant percentage of BB plumes intercepted. Therefore for most of the flights
 11 the Σ PNs methods can be an alternative to identify BB. Moreover, we found that in some flights the
 12 scatter plot between the Σ PNs and the CO (or the HCN and the CO) shows different slopes
 13 identifiable by a pressure threshold, suggesting different regimes between these species that is
 14 different air masses. The dependency of these slopes by the pressure suggested that the air masses
 15 sampled could be spatially (vertically) different and that their origins could be different. Analysing
 16 the back-trajectories, as expected, we found that the air masses were not all originated by biomass
 17 burning and that those at lower pressure (i.e. higher altitude) reach Nova Scotia from the clean
 18 northern region of the Canada. In order to refine the method we adapted an ANN model simulating
 19 the Σ PNs and the HCN in two different ways: 1) using only the CO, NO and CH₃CN as inputs; 2)
 20 adding also the pressure to the inputs. We found that the model results improve in the second case.
 21 In conclusion, we suggest that the Σ PNs can be used as BB tracer for the identification of BB plumes;
 22 moreover, as consequence of the Σ PNs vs CO analysis and of the model results, we suggest that the
 23 use of a meteorological parameter (such as pressure) could allow a better discrimination of the air
 24 masses origin and a more selective method for the selection of BB plumes.

25

26 Acknowledgements

27 The BORTAS project was supported by the Natural Environment Research Council (NERC) under grant
 28 number NE/F017391/1.

29

30 References

31

- 32 Alvarado, M. J., Logan, J. A., Mao, J., Apel E, Riemer, D., Blake, D., Cohen, R. C., Min, K.-E.,
 33 Perring, A. E., Browne, E.C., Wooldridge, P. J., Diskin, G. S., Sachse, G.W., Fuelberg, H.,
 34 Sessions, W. R., Harrigan, D. L., Huey, G., Liao, J., Case-Hanks, A., Jimenez, J. L., Cubison, M.



- 1 J., Vay, S. A., Weinheimer, A. J., Knapp, D. J., Montzka, D. D., Flocke, F. M., Pollack, I. B.,
- 2 Wennberg, P. O., Kurten, A., Crounse, J., St. Clair, J. M., Wisthaler, A., Mikoviny, T., Yantosca,
- 3 R. M., Carouge, C. C., and Le Sager, P.: Nitrogen oxides and PAN in plumes from boreal fires
- 4 during ARCTAS-B and their impact on ozone: an integrated analysis of aircraft and satellite
- 5 observations, *Atmos. Chem. Phys.*, 10, 9739–9760, 2010.
- 6 Andreae, M. O. and Merlet, P.: Emission of trace gases and aerosols from biomass burning, *Global*
- 7 *Biogeochem. Cy.*, 15, 955–966, 2001.
- 8 Biancofiore, F., Verdecchia, M., Di Carlo, P., Tomassetti, B., Aruffo, E., Busilacchio, M., Bianco,
- 9 S., Di Tommaso, S., Colangeli, C.: Analysis of surface ozone using a recurrent neural network,
- 10 *Sci. Total. Environ.*, 514, 379–387, 2015a.
- 11 Biancofiore, F., Busilacchio, M., Verdecchia, M., Tomassetti, B., Aruffo, E., Bianco, S., Di
- 12 Tommaso, S., Colangeli, C., and Di Carlo, P.: Forecasting PM10 and PM2.5 using a recursive
- 13 neural network model, *Atmospheric Res.*, *under review*, 2015b.
- 14 Bertschi, I. T., Jaffe, D. A., Jaegle, L., Price, H. U., and Dennison, J. B.: PHOBEA/ITCT 2002
- 15 airborne observations of trans-Pacific transport of ozone, CO, VOCs, and aerosols to the
- 16 northeast Pacific: Impacts of Asian anthropogenic emissions and Siberian boreal fire emissions,
- 17 *J. Geophys. Res.*, D23S12, doi:10.1029/2003JD004328, 2004.
- 18 Cofer III, W. R., Winstead, E. L., Stocks, B. J., Goldammer, J. G., and Cahoon, D. R.: Crown fire
- 19 emissions of CO₂, CO, H₂, CH₄, and TNMHC from a dense jack pine boreal forest fire,
- 20 *Geophys. Res. Lett.*, 25, 3919–3922, 1998.
- 21 Crutzen, P. J., Andreae, M. O.: Biomass Burning in the Tropics: Impact on Atmospheric Chemistry
- 22 and Biogeochemical Cycles, *Science*, Vol. 250 no. 4988 pp. 1669–1678, 1990.
- 23 Crutzen, P.J., Heidt, L.E., Krasnec, J.P., Pollock W.H., and Seiler, W.: Biomass burning as a source
- 24 of atmospheric gases CO, H₂, N₂O, NO, CH₃Cl and COS. *Nature*, 282, 253–256, 1979.
- 25 Dari-Salisburgo, C., Carlo, P. D., Giammaria, F., Kajii, Y., and D’Altorio, A.: Laser induced
- 26 fluorescence instrument for NO₂ measurements: Observations at a central Italy background
- 27 site, *Atmos. Environ.*, 43, 970–977, 2009.
- 28 Day, D. A., Wooldridge, P. J., Dillon, M. B., Thornton, J. A., and Cohen, R. C.: A thermal dissociation
- 29 laser-induced fluorescence instrument for in-situ detection of NO₂, peroxy nitrates, alkyl nitrates,
- 30 and HNO₃, *J. Geophys. Res.*, 107(D6), 4046, doi:10.1029/2001JD000779, 2002.



- 1 Di Carlo, P., Aruffo, E., Busilacchio, M., Giammaria, F., Dari-Salisburgo, C., Biancofiore, F.,
2 Visconti, G., Lee, J., Moller, S., Reeves, C. E., Bauguitte, S., Forster, G., Jones, R. L., and
3 Ouyang, B.: Aircraft based four-channel thermal dissociation laser induced fluorescence
4 instrument for simultaneous measurements of NO₂, total peroxy nitrate, total alkyl nitrate, and
5 HNO₃, Atmos. Meas. Tech., 6, 971–980, doi:10.5194/amt-6-971-2013, 2013.
- 6 Draxler, R. R.: HYSPLIT4 user's guide, Tech. Rep. NOAA Tech. Memo. ERL ARL-230, NOAA Air
7 Resources Laboratory, Silver Spring, MD, 1999.
- 8 Dibb, J. E., Talbot, R. W., Scheuer, E. M., Seid, G., Avery, M. A., and Singh, H. B.: Aerosol chemical
9 composition in Asian continental outflow during the TRACE-P campaign: Comparison with
10 PEM-West B, J. Geophys. Res., 108(D21), 8815, doi:10.1029/2002JD003111, 2003.
- 11 Elman LJ.: Finding structure in time. Cognitive Science. 14, 179–211, 1990.
- 12 Gerbig, C., Schmitgen, S., Kley, D., Volz-Thomas, A., Dewey, K., and Haaks, D.: An improved fast-
13 response vacuum-UVresonance fluorescence CO instrument, J. Geophys. Res., 104 (D1), 1699–
14 1704, 1999.
- 15 Gillett, N., Weaver, A. J., Zwiers, F. W., and Flannigan, M. D.: Detecting the effect of climate change
16 on Canadian forest fires, Geophys. Res. Lett., 31, L18211, doi:10.1029/2004GL020876, 2004.
- 17 Goode, J. G., Yokelson, R. J., Ward, D. E., Susott, R. A., Babbitt, R. E., Davies, M. A., and Hao, W.
18 M.: Measurements of Excess O₃, CO₂, CO, CH₄, C₂H₄, C₂H₂, HCN, NO, NH₃, HCOOH,
19 CH₃COOH, HCHO and CH₃OH in 1997 Alaskan Biomass Burning Plumes by Airborne Fourier
20 Transform Infrared Spectroscopy (AFTIR), J. Geophys. Res., 105, 22147–22166, 2000.
- 21 Holzinger, R., Williams, J., Salisbury, G., Klupfel, T., de Reus, M., Traub, M., Crutzen, P. J., and
22 Lelieveld, J.: Oxygenated compounds in aged biomass burning plumes over the Eastern
23 Mediterranean: evidence for strong secondary production of methanol and acetone, Atmos.
24 Chem. Phys., 5, 39–46, 2005.
- 25
- 26 Hopkins, J. R., Read, K. A., and Lewis, A. C.: Two column method for long-term monitoring of non-
27 methane hydrocarbons (NMHCs) and oxygenated volatile organic compounds, J.
28 Environ. Monitor., 5, 8–13, 2003.
- 29 Hornbrook, R. S., Blake, D. R., Diskin, G. S., Fried, A., Fuelberg, H. E., Meinardi, S., Mikoviny, T.,
30 Richter, D., Sachse, G. W., Vay, S. A., Walega, J., Weibring, P., Weinheimer, A. J., Wiedinmyer,
31 C., Wisthaler, A., Hills, A., Riemer, D. D., and Apel, E. C.: Observations of nonmethane organic



- 1 compounds during ARCTAS –Part 1: Biomass burning emissions and plume enhancements,
- 2 Atmos. Chem. Phys., 11, 11103–11130, 2011.
- 3 Hudman, R.C., Jacob, D.J., Turquety, S., Leibensperger, E.M., Murray, L.T., Wu, S., Gilliland, A.,
- 4 Avery, M., Bertram, T., Brune, W., Cohen, R., Dibb, J., Flocke, F., Fried, A., Holloway, J.,
- 5 Neuman, J., Orville, R., Perring, A., Ren, X., Sachse, G., Singh, H., Swanson, A., and
- 6 Wooldridge, P.: Surface and lightning sources of nitrogen oxides over the United States:
- 7 Magnitudes, chemical evolution, and outflow, J. Geophys. Res., 112, D12S05,
- 8 doi:10.1029/2006JD007912, 2007.
- 9 Jacob, D. J., Wofsy, S. C., Bakwin, P. S., Fan, S.-M., Harriss, R.C., Talbot, R.W., Bradshaw, J.,
- 10 Sandholm, S., Singh, H. B., Gregory, G. L., Browell, E. V., Sachse, G. W., Blake, D. R., and
- 11 Fitzjarrald, D. R.: Summertime photochemistry at high northern latitudes, J. Geophys. Res., 97,
- 12 16421–16431, 1992.
- 13 Jaffe, D.A., and Wigder, N.L.: Ozone production from wildfires: A critical review. Atmospheric
- 14 Environment 51, 1–10, doi:10.1016/j.atmosenv.2011.11.063, 2012.
- 15 Lavoué D., Liousse C., Cachier H., Stocks B.J., and Goldammer J.G.: Modeling of carbonaceous
- 16 particles emitted by boreal and temperate wildfires at northern latitudes. J. Geophys. Res.:
- 17 Atmos. 105(D22): 26871–26890, 2000.
- 18 Le Breton, M., Bacak, A., Muller, J. B. A., O'Shea, S. J., Xiao, P., Ashfold, M. N. R., Cooke, M. C.,
- 19 Batt, R., Shallcross, D. E., Oram, D. E., Forster, G., Bauguitte, S. J.-B., Palmer, P. I.,
- 20 Parrington, M., Lewis, A. C., Lee, J. D., and Percival, C. J.: Airborne hydrogen cyanide
- 21 measurements using a chemical ionisation mass spectrometer for the plume identification of
- 22 biomass burning forest fires, Atmos. Chem. Phys., 13, 9217–9232, doi:10.5194/acp-13-9217-
- 23 2013, 2013.
- 24 Lee, J. D., Moller, D. J., Read, K. A., Lewis, A. C., Mendes, L., and Carpenter, L. J.: Year-round
- 25 measurements of nitrogen oxides and ozone in the tropical North Atlantic marine boundary layer,
- 26 J. Geophys. Res., 114, D21302, doi:10.1029/2009JD011878, 2009
- 27 Leung, F.-Y. T., Logan, J. A., Park, R., Hyer, E., Kasischke, E., Streets, D., and Yurganov, L.: Impacts
- 28 of enhanced biomass burning in the boreal forests in 1998 on tropospheric chemistry and the
- 29 sensitivity of model results to the injection height of emissions, J. Geophys. Res., 112, D10313,
- 30 doi:10.1029/2006JD008132, 2007.
- 31 Lewis, A. C., Evans, M. J., Methven, J., Watson, N., Lee, J. D., Hopkins, J. R., Purvis, R. M., Arnold,
- 32 S. R., McQuaid, J. B., Whalley, L. K., Pilling, M. J., Heard, D. E., Monks, P. S., Parker, A. E.,



- 1 Reeves, C. E., Oram, D. E., Mills, G., Bandy, B. J., Stewart, D., Coe, H., Williams, P., and
- 2 Crosier, J.: Chemical composition observed over the mid-Atlantic and the detection of pollution
- 3 signatures far from source regions, *J. Geophys. Res.*, 112, D10S39, doi:10.1029/2006JD007584,
- 4 2007.
- 5 Lewis, A. C., Evans, M. J., Hopkins, J. R., Punjabi, S., Read, K. A., Purvis, R. M., Andrews, S. J.,
- 6 Moller, S. J., Carpenter, L. J., Lee, J. D., Rickard, A. R., Palmer, P. I., and Parrington, M.: The
- 7 influence of biomass burning on the global distribution of selected non-methane organic
- 8 compounds, *Atmos. Chem. Phys.*, 13, 851–867, www.atmos-chem-phys.net/13/851/2013/, 2013.
- 9 Lonbladd L., Peterson C., and Röngvaldsson T.: Pattern recognition in high energy physics with
- 10 artificial neural network – Jetnet 2.0., *Comput. Phys. Comm.* 70, 167–182, 1992.
- 11 Marlon, J. R., Bartlein, P. J., Carcaillet, C., Gavin, D. G., Harrison, S. P., Higuera, P. E., Joos,
- 12 F., Power, M. J., and Prentice, I. C.: Climate and human influences on global biomass burning
- 13 over the past two millennia, *Nature Geoscience*, 1, 69–702, 2008.
- 14 Mauzerall, D., Jacob, D. J., Fan, S.-M., Bradshaw, J., Gregory, G., Sachse, G., and Blake, D.: Origin
- 15 of tropospheric ozone at remote high northern latitudes in summer, *J. Geophys. Res.*, 101, 4175–
- 16 4188, 1996.
- 17 Murphy, J. G., Oram, D. E., and Reeves, C. E.: Measurements of volatile organic compounds over
- 18 West Africa, *Atmos. Chem. Phys.*, 10, 5281–5294, doi: 10.5194/acp-10-5281-2010, 2010.
- 19 O’Shea, S. J., Allen, G., Gallagher, M. W., Bauguitté, S. J.-B., Illingworth, S. M., Le Breton, M.,
- 20 Muller, J. B. A., Percival, C. J., Archibald, A. T., Oram, D. E., Parrington, M., Palmer, P. I., and
- 21 Lewis, A. C., Airborne observations of trace gases over boreal Canada during BORTAS:
- 22 campaign climatology, air masses analysis and enhancement ratios, *Atmos. Chem. Phys.*, 13,
- 23 12451–12467, 2013.
- 24 Palmer, P. I., Parrington, M., Lee, J. D., Lewis, A. C., Rickard, A. R., Bernath, P. F., Duck, T. J.,
- 25 Waugh, D. L., Tarasick, D. W., Andrews, S., Aruffo, E., Bailey, L. J., Barrett, E., Bauguitté, S.
- 26 J.-B., Curry, K. R., Di Carlo, P., Chisholm, L., Dan, L., Forster, G., Franklin, J. E., Gibson, M.
- 27 D., Griffin, D., Helmig, D., Hopkins, J. R., Hopper, J. T., Jenkin, M. E., Kindred, D., Kliever,
- 28 J., Le Breton, M., Matthiesen, S., Maurice, M., Moller, S., Moore, D. P., Oram, D. E., O’Shea, S.
- 29 J., Owen, R. C., Pagnello, C. M. L. S., Pawson, S., Percival, C. J., Pierce, J. R., Punjabi, S., Purvis,
- 30 R. M., Remedios, J. J., Rothermund, K. M., Sakamoto, K. M., da Silva, A. M., Strawbridge, K. B.,
- 31 Strong, K., Taylor, J., Trigwell, R., Tereszchuk, K. A., Walker, K. A., Weaver, D., Whaley, C.,
- 32 and Young, J. C.: Quantifying the impact of Boreal forest fires on Tropospheric oxidants over



- 1 the Atlantic using Aircraft and Satellites (BORTAS) experiment: design, execution and science
- 2 overview, *Atmos. Chem. Phys.*, 13, 6239–6261, doi:10.5194/acp-13-6239-2013, 2013.
- 3 Parrington, M., Palmer, P. I., Henze, D. K., Tarasick, D. W., Hyer, E. J., Owen, R. C., Helmig, D.,
- 4 Clerbaux, C., Bowman, K. W., Deeter, M. N., Barratt, E. M., Coheur, P.-F., Hurtmans, D., Jiang,
- 5 Z., George, M., and Worden, J. R.: The influence of boreal biomass burning emissions on the
- 6 distribution of tropospheric ozone over North America and the North Atlantic during
- 7 2010, *Atmos. Chem. Phys.*, 12, 2077–2098, doi:10.5194/acp-12-2077-2012, 2012.
- 8 Purvis, R. M., Lewis, A. C., Hopkins, J. R., Andrews, S., and Minaeian, J.: Functionalized aromatic
- 9 compounds within middle troposphere boreal biomass burning plumes, in preparation, 2013.
- 10 Real, E., Law, K. S., Weinzierl, B., Fiebig, M., Petzold, A., Wild, O., Methven, J., Arnold, S., Stohl,
- 11 A., Huntrieser, H., Roiger, A., Schlager, H., Stewart, D., Avery, M., Sachse, G., Browell, E.,
- 12 Ferrare, R., and Blake, D.: Processes influencing ozone levels in Alaskan forest fire plumes
- 13 during long-range transport over the North Atlantic, *J. Geophys. Res.*, 112,
- 14 D10S41, doi:10.1029/2006JD007576, 2007.
- 15 Reid, J. S., Hyer, E. J., Prins, E. M., Westphal, D. L., Zhang, J., Wang, J., Christopher, S. A., Curtis,
- 16 C. A., Schmidt, C. C., Eleuterio, D. P., Richardson, K. A., and Hoffman, J. P.: Global monitoring
- 17 and forecasting of biomass burning smoke: Description of and lessons from the Fire Locating and
- 18 Modeling of Burning Emissions (FLAMBE) program, *IEEE J. Sel. Top. Appl.*, 2, 144–162, 2009.
- 19 Reidmiller, D. R., Jaffe, D. A., Fischer, E. V., and Finley, B.: Nitrogen oxides in the boundary layer
- 20 and free troposphere at the Mt. Bachelor Observatory, *Atmos. Chem. Phys.*, 10, 6043–
- 21 6062, doi:10.5194/acp-10-6043-2010, 2010.
- 22 Rinsland, C. P., Dufour, G., Boone, C. D., Bernath, P. F., Chiou, L., Coheur, P.-F., Turquety, S., and
- 23 Clerbaux, C.: Satellite boreal measurements over Alaska and Canada during June–July 2004:
- 24 Simultaneous measurements of upper tropospheric CO, C₂H₆, HCN, CH₃Cl, CH₄, C₂H₂,
- 25 CH₃OH, HCOOH, OCS, and SF₆ mixing ratios, *Global Biogeochemical Cycles*, Vol. 21,
- 26 GB3008, doi:10.1029/2006GB002795, 2007.
- 27 Tereszchuk, K. A., Gonzalez Abad, G., Clerbaux, C., Hurtmans, D., Coheur, P.-F., and Bernath, P.
- 28 F.: ACE-FTS measurements of trace species in the characterization of biomass burning plumes,
- 29 *Atmos. Chem. Phys.*, 11, 12169–12179, 2011.
- 30 Vay, S. A., Choi, Y., Vadrevu, K. P., Blake, D. R., Tyler, S. C., Wisthaler, A., Hecobian, A., Kondo,
- 31 Y., G. S. Diskin, G. S., Sachse, G. W., Woo, J.-H., Weinheimer, A. J., Burkhardt, J. F., Stohl, A.,
- 32 and Wennberg, P. O.: Patterns of CO₂ and radiocarbon across high northern latitudes during



- 1 International Polar Year 2008 , J. Geophys. Res., 116, D14301, doi:10.1029/2011JD015643,
- 2 2011.
- 3 Val Martin, M., Honrath, R., Owen, R. C., Pfister, G., Fialho, P., and Barata, F.: Significant
- 4 enhancements of nitrogen oxides, ozone and aerosol black carbon in the North Atlantic lower
- 5 free troposphere resulting from North American boreal wildfires, J. Geophys. Res., 111, D23S60,
- 6 doi:10.1029/2006JD007530, 2006.
- 7 Wilson, K. L. and Birks, J. W.: Mechanism and Elimination of a Water Vapor Interference in the
- 8 Measurement of Ozone by UV Absorbance, Environmental Science and Technology 40, 6361-
- 9 6367,2006.
- 10 Wofsy, S.C., Sachse, G.W., Gregory, G.L., Blake, D.R., Bradshaw, J.D., Sandholm, S.T., Singh,
- 11 H.B., Barrick, J.A., Harriss, R.C., Talbot, R.W., Shipham, M.A., Browell, E.V., Jacob, D.J. and
- 12 Logan, J.A.:Atmospheric chemistry in the Arctic and subarctic: Influence of natural fires,
- 13 industrial emissions, and stratospheric inputs. J. Geophys. Res., 97: doi: 10.1029/92JD00622.
- 14 issn: 0148-0227, 1992.
- 15 Wotawa, G., and Trainer, M.:The influence of Canadian forest fires on pollutant concentrations in
- 16 the United States. Science 288(5464):324-328, 2000.

17